Food Hydrocolloids 150 (2024) 109663

Contents lists available at ScienceDirect

Food Hydrocolloids

journal homepage: www.elsevier.com/locate/foodhyd

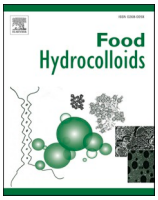

Extrapolation of classical rheometry of plant protein pastes to extrusion conditions

R.G.M. van der Sman *, P. Voudouris, J.R. Hamoen

Wageningen Food & Biobased Research, the Netherlands

ARTICLE INFO

Keywords:
Rheology
Superposition
Glass transition
Plant protein

ABSTRACT

This study explores alternative methods to measure the rheology of pastes based on soy and pea proteins, which are commonly used as starting material in extrusion for the preparation of meat analogs. Currently, it is still a challenge to obtain consistent rheological data on such materials for steady shear at conditions that are relevant for the extrusion of such systems. Hence, possibilities are explored for the extrapolation of results obtained with classical rheometers operating at temperatures below boiling point, to conditions that are relevant for the extrusion of such systems. The above was combined, with findings from off-line and in-line capillary rheometers, which can provide steady shear measurements above boiling point and at hydration levels as used in extrusion.

We have analysed the consistency of our new results with previous oscillatory shear measurements, performed at conditions similar to those of meat analog extrusion. For validation of the extrapolation we have analysed whether the new rheology data follow similar scaling rules. As classical rheometers can handle only moderate torques, the measurements are limited to hydration levels higher than those used in extrusion (75–85%). Despite this limitation, strain sweeps with classical rheometers show that in this regime the elastic modulus also scales with T_g/T, the ratio of glass transition, and actual temperature. Yet, its dependency on T_g/T appears differently from measurements performed at extrusion-like conditions. Moreover, our current results indicate a strong thixotropic nature of plant protein pastes at temperatures below boiling point. Consequently, flow curves are only stable if performed from high to low shear rates. Nevertheless, our data can be mapped to a single master curve following the Herschel-Bulkley model, with parameters also following a scaling rule dependent on T_g/T.

This T_g/T scaling is used to construct master curves with data from the off-line and in-line capillary rheometers. The obtained shift factors for the flow curves are in agreement with old literature data obtained for SPI, but they deviate significantly from our steady shear measurements with classical rheometers. Based on the results of our current and previous study we have a critical, general discussion on the possibility of extrapolation of classical rheometry of plant protein pastes to process conditions used for production of meat analogs.

1. Introduction

Knowledge of rheology characteristics of plant protein pastes is important for the development of meat analogs, manufactured via extrusion or shear cell technology. Recent results as obtained with the Closed Cavity Rheometer (CCR), via which performed both frequency and strain sweeps at temperatures above the boiling point of water (van der Sman, Chakraborty, Hua, & Kollmann, 2023) provided insights on the rheological behaviour of such systems. These elevated temperatures are used during the manufacturing of meat analogs (Cornet, Snel, et al., 2020). For foods in classical rheometers the boiling point is the upper bound for the operating temperature, as the water in the food will boil off, and escape from the rheometer. This problem is solved with the CCR via the use of a sealed, closed cavity containing the food paste. Via the application of a normal force on the cavity, the rheometer can withstand pressures up to 4 bars, allowing measurements up to 140^{o}C. As the CCR is developed for rubbers, it is supplied with a motor that can generate higher torques than a classical rheometer. Furthermore, via grooves in the cavity wall, wall slip is reasonably prevented. Hence, it can handle plant protein doughs with relatively low moisture contents down to 45%. As such the CCR has been propagated by others for the study of the rheology of meat analogs (Pietsch, Bühler, Karbstein, & Emin, 2019; Schreuders et al., 2021; Schreuders et al., 2022; Wittek, Zeiler, Karbstein, & Emin, 2020; Wittek, Walther, Karbstein, & Emin, 2021). Yet, the

* Corresponding author.
E-mail address: ruud.vandersman@wur.nl (R.G.M. van der Sman).

https://doi.org/10.1016/j.foodhyd.2023.109663
Received 6 June 2023; Received in revised form 4 December 2023; Accepted 16 December 2023
Available online 19 December 2023

CCR is limited to only oscillatory shear - while during extrusion meat analogs flow under steady shear.

Because there is still an open research question on how to translate results from oscillatory rheology to steady shear conditions, one can not transform CCR to steady shear conditions as occurs during meat analog manufacturing. Typically, plant protein pastes can be measured under steady shear via a) classical rheometer, but at temperatures below boiling point and low torques, and b) capillary rheometer at high temperatures above boiling point and high shear rates. However, capillary rheometer results can be plagued by entry effects, and wall slip (Corfield, Adams, Briscoe, Fryer, & Lawrence, 1999; Martin, Odic, Russell, Burns, & Wilson, 2008). Via extensive, extra measurements one could correct for these effects. Moreover, one can not measure yield stresses with them. Knowledge of yield stresses is important for meat analogs, as they determine the liquid-to-solid transition in the cooling die (van der Sman & van der Goot, 2023). Yet, yield stresses can be directly measured via classical rheometers. Thus, in this paper, we explore whether via combined measurements of classical and capillary rheometry, one can sufficiently characterize the steady shear rheology of plant proteins used for meat analogs.

Classical rheometers can provide accurate measurements, but as provided previously the temperature is limited to boiling point. Typically torques from classical rheometers are lower than the CCR, corresponding that the range of moisture content will be limited to values higher than used in high-moisture-extrusion. In our previous study, we have demonstrated that rheological properties like elastic modulus and relaxation time (shift factors) follow scaling laws with T_g/T, the ratio of the (moisture-dependent) glass transition temperature (T_g), and the actual temperature (T). Via this parameter, one can construct master curves of rheological responses of protein doughs (van der Sman et al., 2023), but also of carbohydrates, maltodextrins, and starch (van Der Sman, 2013; van der Sman & Mauer, 2019; van der Sman, Ubbink, Dupas-Langlet, Kristiawan, & Siemons, 2021; Siemons, Veser, Boom, Schutyser, & van der Sman, 2022). Via the constructed master curves, and shift factors depending on T_g/T, rheological properties to regimes, which lie outside the measured range of temperatures and moisture contents can be constructed. In this study, we investigate whether with the help of constructed master curves results obtained with the classical rheometers can be translated to the more intensive extrusion conditions. Measurements are performed for soy and pea protein isolates as model systems for meat analog applications. Here, is investigated the behaviour of SPI and SPC via off-line and in-line capillary rheometers. It is noted that uncorrected results from capillary rheometers can still be used for the investigation of scaling rules and construction of master curves (Cardinaels, Van Puyvelde, & Moldenaers, 2007; van der Sman et al., 2021). We identify scaling rules that are compared to the results obtained with the classical rheometer, as mentioned above, and the CCR results from our previous study (van der Sman et al., 2023) to similar plant-based past systems. the results from this study are also compared to other literature capillary rheometer data for SPI from literature (Fujio, Hayashi, & Hayakawa, 1991; Hayashi, Hayakawa, & Fujio, 1991, 1992, 1993).

This study is concluded with a general discussion on the measurement of the rheology of meat analogs, based on our previous and current results and insights from other recent studies on meat analog (rheology).

2. Materials and methods

2.1. Oscillation and shear rheology

Rheological characteristics of pea and soy protein isolates were measured at different temperatures $70 \leq T \leq 100^oC$, with solids concentrations of 15, 20, 25%. We have used commercial ingredients: soy protein isolates (SPI) (SUPRO 500E IP, Danisco Solae, having 94% dry matter composed of 90% protein, 1% fat, and 5% ash (Jia, Rodriguez-Alonso, Bianeis, Keppler, & van der Goot, 2021)) and yellow pea protein isolate (PPI) (Nutralys F85G with 84% protein, 1% dietary fibre, 9% lipids, and 4% ash (Schreuders et al., 2022)). Aqueous pastes of proteins were prepared with distilled water. The water was added to the protein powder and mixed thoroughly with a spatula for about 5 min. After mixing, all protein pastes were allowed to equilibrate at room temperature for 30 min before they were measured in the rheometer. The preparation step is similar to the preparation step used in our previous research on which the importance of hydration of protein pastes for meat analogs is highlighted (Cornet, Snel, et al., 2020). The hydration time is taken equal to that applied in meat analog production via shear-cell technology (Grabowska, Tekidou, Boom, & van der Goot, 2014). As in the case of the shear-cell the hydration is performed before the shearing. Consequently, moisture transport is only via diffusion. For the case of extrusion, hydration is performed within the screw section (van der Sman & van der Goot, 2023), where it is driven by both diffusion and convection due to the shearing. Hence, the hydration in extruders is much more intensive. However, because of the similarities between meat analog products produced with shear cell technology and extrusion, we assume that the overall effect of the two hydration schemes is comparable.

Rheological characterizations were performed using a TA Instrument Discovery Hybrid Rheometer equipped with a solvent trap. The samples were placed in a concentric cylinder geometry, with a grooved bob diameter and length of 14 mm and 21 mm respectively, and subjected to the following protocol: A time sweep for 10 min 95^{o}C at 1% strain and a frequency of 1 Hz. This step was applied as a conditioning step, before the actual measurements. While expecting that most proteins have already been denatured via the preprocessing at the manufacturer, in line with our previous work, we nevertheless used this pre-treatment step to ensure that all proteins are in the denatured state (van der Sman et al., 2023). Following this pretreatment, another time sweep of 10 min was applied, at the same set strain and frequency values, to equilibrate the sample at the temperature of interest e.g. $70 \leq T \leq 100^oC$. The protocol then includes a strain sweep from 0.01% up to 500% and subsequently a reverse strain sweep from 500% down to 0.01%. Sweeps are performed at different frequencies in the range {0.1, 0.5, 1.0, 5.0} Hz. Flow curves are measured in two cycles, with each cycle we let the shear rates go up ($0.1–500s^{-1}$) and down ($500\text{-}0.1s^{-1}$). In between the two flow curve cycles, are performed the amplitude sweeps, as described previously. For selected samples we measured the moisture content before and after the end of the above-described experimental protocol, and we found no significant differences. Hence, the loss of moisture during measurement is negligible.

2.2. Capillary rheology

For capillary rheometry was used soy protein concentrate (SPC) (Alpha 8, Solae, 96% dry matter composed of 70% protein, 2% fat, 7% ash, 18% dietary fiber, and total carbohydrates of 19.6% (Jia et al., 2021)). The samples were measured after the SPC was processed with the extruder (without cooling die, but with little expansion) at different moisture content $50 \leq MC \leq 60\%$. A high-pressure capillary rheometer (RG25, Goettfert, Buchen, Germany) was operated in the controlled speed mode to consecutively measure shear viscosities in the apparent shear rate range $50–5000s^{-1}$. Experiments were done in the temperature range $95 \leq T \leq 120^oC$. All the capillary measurements were repeated twice to ensure data reproducibility. Three circular dies of diameter D = 1 mm and D = 2 mm and different lengths L = 15 and L = 30 mm were used. Capillary rheology of SPI was not successful because of blockage of the capillary. Based on laboratory experience attribute this to the strong adhesion of protein isolates to the capillary wall, which is reduced in the presence of fibers. A similar hypothesis is posed for adhesives based on soy (Sadare, Daramola, & Afolabi, 2020).

2.3. Inline rheometry

A Twinlab-F 20/40 co-rotating double screw extruder (Brabender, Duisburg) was used to produce high-moisture plant-based extrudates. At the die-adapter, between the barrel and die, a ViscoIndicator Online Rheometer (Dynisco Europe GmbH, Heilbronn) was connected to the extruder, as shown in Fig. 1.

The ViscoIndicator consists of a rotary pump, a product chamber, and a capillary. A pressure sensor was connected to the chamber. The tube between the extruder and the ViscoIndicator was as short as possible. This tube and the different parts of the ViscoIndicator were heated up to the actual temperature at the die adapter. The shear rate in the capillary can be varied via the speed of the rotary pump. The protein powder was fed to the extruder using a gravimetric feeder (Brabander, DDW-M-DDSR20) at the first inlet, while water was added via a hose pump (Watson Marlow, 120U) in the second inlet (see Fig. 2).

The shear stress is calculated from the pressure sensor signal. Data was recorded after the signal had reached a steady value. Inline rheometry was performed with soy protein concentrate with moisture content in the range {50, 55, 60}%, and with soy protein isolate having a moisture content of 55%.

The extrusion process was performed with a feed of 6 kg/h. The screw speed varied between 250 and 1200 rpm. For temperature control, the screw section is divided into four equal sections, whose temperature can be controlled independently. The temperature of the first two sections (I & II) was fixed at 40 and 80^{o}C. The third section was 100 or 110^{o}C. The last section (IV) was either 110, 120, 130, or 140^{o}C.

2.4. Scaling rules and master curves

In previous studies, we have shown that several rheological parameters of biopolymers scale with T_g/T, such as the elastic modulus in the linear viscoelastic regime G_N, zero shear viscosity η_0, and relaxation times $\tau \sim \eta_0/G_N$. Here is analysed whether the rheology of protein pastes below boiling point temperature, $T < 373$ K, as measured with the classical rheometers, also scale with this parameter. Fig. 3 indicates the experimental conditions of this study and our previous study (van der Sman et al., 2023) in a contour plot of T_g/T for pea proteins. The value of T_g/T under the current experimental conditions is in a similar range as normal extrusion conditions, where $T \approx 140^o$C (413 K) and $MC \approx 50\%$.

Master curves are constructed for the strain sweeps, via scaling both the elastic and loss moduli, G' and G'', with the elastic modulus in the linear viscoelastic (LVE) regime G_N. In line with our previous study (van der Sman et al., 2023), we expect that the critical strain γ_{cr}, determining the end of the LVE, is independent of moisture and temperature. Beyond the critical strain, the protein paste shows strain softening, following a power law, $G' \sim \gamma^{-\nu_1}$, and $G'' \sim \gamma^{-\nu_2}$. The horizontal axis is rescaled with the critical strain γ_{cr}. The critical strain is determined by fitting the following descriptive model:

$$\begin{aligned} G'/G_N &= \left[1+\left(\frac{\gamma}{\gamma_{cr}}\right)^a\right]^{2(n-1)/a} \\ G''/G_N &= \tan(\delta)\left[1+\left(\frac{\gamma}{\gamma_{cr}}\right)^a\right]^{(n-1)/a} \end{aligned} \tag{1}$$

The above model is inspired by the Carreau-Yasuda model for viscosity, which has been applied already in our previous study (van der Sman et al., 2023), where we have determined that $a = 1.5$. Note, that the above model implies $\nu_1/\nu_1 = 2$, similar to observations for other soft matter systems (Derec, Ducouret, Ajdari, & Lequeux, 2003; Miyazaki, Wyss, Weitz, & Reichman, 2006; Mohan, Pellet, Cloitre, & Bonnecaze, 2013; Pellet & Cloitre, 2016). For meat analogs, the following hypothesis is posed (van der Sman et al., 2023):

$$\tan(\delta) = \tan(n\pi/2) \tag{2}$$

As horizontal shift factor is reported $a_T = \gamma_{cr}/\gamma_{cr,ref}$, with $\gamma_{cr,ref}$ the critical strain at (arbitrary) reference conditions. G_N can be viewed as a vertical shift factor. Via rescaling with these shift factors it has been constructed master curves of the experimental data, concerning the strain sweeps. Finally, we note that the above formulation, Eq. (1), is phenomenological, but needs to be reflected against theory. Most importantly it lacks a description of weak strain overshoot, as observed in our previous study (van der Sman et al., 2023).

Under steady flow conditions, as flow curves are measured with the classical rheometers or performing capillary rheometry, is expected the protein pastes to follow the Herschel-Bulkey model (van der Sman et al., 2023), similar to previous studies of others (Hayashi, Hayakawa, & Fujio, 1993; Högg, Horneber, & Rauh, 2017; Morgan, Steffe, & Ofoli, 1989):

$$\sigma = \sigma_Y\left[1+\left(\frac{\dot\gamma}{\dot\gamma_{cr}}\right)^m\right] \tag{3}$$

Here σ_Y is the yield stress, $\dot\gamma_{cr}$ a critical shear rate, and m the shear thinning exponent. Based on our previous study is expected that $\sigma_Y \sim G_N\gamma_{cr}$, and m to be related to n (van der Sman et al., 2023).

The existence of a critical strain, γ_{cr}, independent of temperature, protein content, and frequency, implies the following scaling of the Herschel-Bulkley model parameters (Gibouin, van der Sman, Benedito, & Della Valle, 2022):

$$\sigma_Y = \tilde\sigma_Y a_T \dot\gamma_{cr} = \tilde{\dot\gamma}_{cr} a_T \tag{4}$$

$\tilde\sigma_Y$, and $\tilde{\dot\gamma}_{cr}$ are parameter values at (arbitrary) reference conditions, and a_T is the shift factor. Hence, for the construction of a master flow curve, is expected the horizontal and vertical shift factors to be inversely proportional. Moreover, as $\sigma_Y = G_N\gamma_{cr}$, the a_T scales similar with T_g/T as G_N.

The master curves of the flow curve data are obtained by fitting the Herschel-Bulkley model to individual curves and rescaling the experimental data with σ_Y and $\dot\gamma_{cr}$.

The above rescaling is often difficult to perform for capillary rheometry, as the experimental data often lack the regime showing well-defined yield stress (Hayashi et al., 1993; Morgan et al., 1989). Furthermore, to obtain true stresses and shear rates, corrections have to be performed on the raw data of the capillary rheometer (Jebalia, Della Valle, & Kristiawan, 2022). Traditionally, the Rabinowitch correction is applied to the apparent shear rate, and the Bagley correction for the entrance pressure is applied to obtain the true wall stress. At large L/$D >$ 10 ratios the entrance pressure is often much smaller than the total pressure (Jebalia et al., 2022).

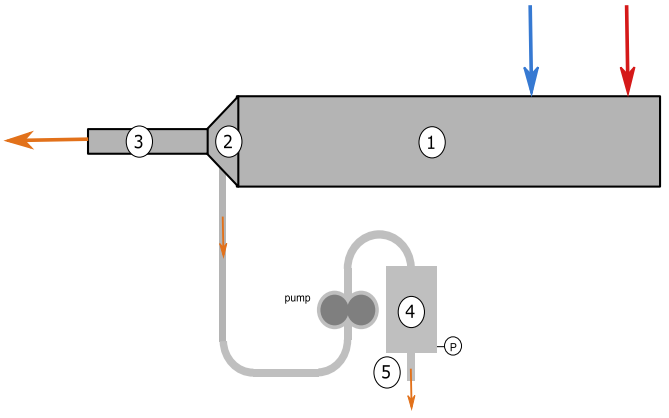

Fig. 1. Schematic drawing of the experimental setup for the inline rheometry. (1) the extruder, (2) the barrel adaptor, (3) the cooling die, (4) the ViscoIndicator, and (5) the measurement capillary, before which the pressure (p) is measured. A small side stream is drawn from the barrel adaptor via the feeding pump, forcing it through the measurement capillary (5).

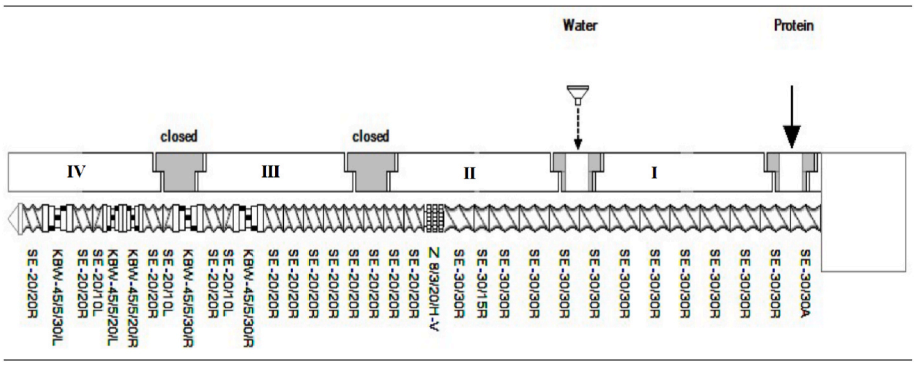

Fig. 2. Setup of the barrel section of the Brabender extruder, showing the screw configuration with the different Brabender screw elements, and the inlet ports of protein powder and water. Material flows from right to left. Sections I-IV can be heated to different temperatures.

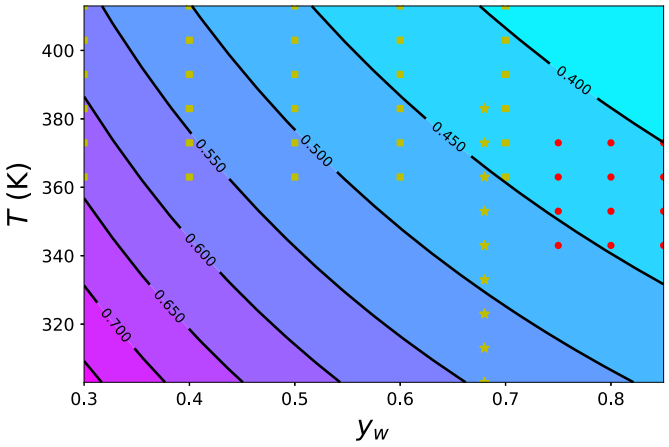

Fig. 3. Experimental conditions in terms of moisture content (y_w) and temperature (T) indicated in a contour plot indicating the T_g/T values for pea protein. Red dots indicate experimental conditions for the classical rheometer methods, and the yellow symbols indicate the experimental conditions used in the CCR experiments performed in our previous study (van der Sman et al., 2023).

However, at stress sufficiently larger than the yield stress, the protein pastes can be approximated as a power-law fluid, with $\sigma \sim \dot{\gamma}^m$. Hence, for negligible entrance pressure, the Rabinowitch correction implies that the apparent wall stress and apparent shear rate follow the same scaling as the true stress and shear rate: $\sigma_{app} \sim \dot{\gamma}^m_{app}$ (Jebalia et al., 2022; Swallow, 2002). Consequently, a master curve is constructed using the (apparent) wall shear stress versus (apparent) shear rate, via simultaneous vertical and horizontal shifting:

$$\widetilde{\sigma} = \sigma \Big/ a_T \;\; ; \;\; \widetilde{\dot{\gamma}} = \dot{\gamma} a_T \tag{5}$$

As above, a linear relation is assumed between the logarithmic shift factor $\log(a_T)$ and T_g/T, cf. (van der Sman et al., 2023).

$$\log(a_T) = p_1 + p_2 \frac{T_g}{T} \tag{6}$$

The two coefficients p_1 and p_2 are determined by minimizing the distance between rescaled curves, in a least squares sense.

The procedure is applied to both SPI and SPC. For estimating T_g of SPC we rely on the observation by the study (Kyomugasho, Kamau, Aravindakshan, & Hendrickx, 2021) that $T_{g,s}$ of cell wall materials is similar to soy proteins ($T_{g,s} = 387$ K). Hence, is assumed that T_g of SPC follows a similar relation as for SPI, in line with our previous study, which is shown to follow Couchman-Karasz (van der Sman et al., 2023).

In the general discussion, is investigated the consistency of data obtained from this study with literature data of viscosity measured at various conditions. The literature data is also rescaled following the procedure of Della Valle for the shear-thinning viscosity (Kristiawan, Chaunier, Della Valle, Lourdin, & Guessasma, 2016; Valle, Vergnes, & Lourdin, 2007):

$$\frac{\eta}{a_T} = f(\dot{\gamma} a_T) \tag{7}$$

This rescaling has been applied earlier to shear thinning starches and maltodextrins (van der Sman et al., 2021). It is shown that this shift factor is equal to the zero shear viscosity, and thus a function of T_g/T. The assumption that is made is that it also holds for the viscosity of the investigated protein paste.

3. Results

3.1. Strain sweeps

3.1.1. Pea proteins

Using the data from the sweep from low to high strain (up-sweep), a master curve is constructed via normalizing G' and G'' with the average elastic modulus G_0, holding in the linear regime $0.1 < \gamma < 1\%$. Slight horizontal shifting was performed via rescaling with γ_{cr}. Exemplary strain sweeps are provided in the left pane of Fig. 4, which indicates that there is some weak strain overshoot at the crossover point.

The master curve is shown in the right pane of Fig. 4, which is fitted to the model presented in the theoretical section. The data are fitted with $a = 1.5$, and $n = 0.175$.

The horizontal and vertical shift factors a_T and G_N are plotted as a function of T_g/T in Fig. 5. The average horizontal shift factor is about unity, $a_T \approx 1$, except for two outliers and it does not have a strong correlation with frequency. This supports the hypothesis that there is a critical strain quite independent of temperature, protein concentration, and frequency (van der Sman et al., 2023). For the plateau modulus G_N versus T_g/T, there is a scattering of data but there is an increase with T_g/T.

Subsequently, the data from strain sweep from high to low strains (down-sweep) were analysed. This provides information about dynamic yield stresses/related to thixotropy.

A master curve was constructed based only on the down-sweep data, using only the low frequencies (f = 0.1 and 0.5 Hz). Exemplary downward sweeps are given in the left pane of Fig. 6, while the right pane shows the constructed master curve. The shift factors are shown in Fig. 7. In Fig. 6 the fitted curve from Fig. 4 is repeated so the differences between upward and downward sweeps are more visible.

For that, the horizontal shift factors are observed to follow the trend of Fig. 5, where $a_T \approx 1$, but there is much more scatter. Via the comparison with the fitted upward master curve, we can conclude that the critical strain is similar for both upward and downward strain sweeps.

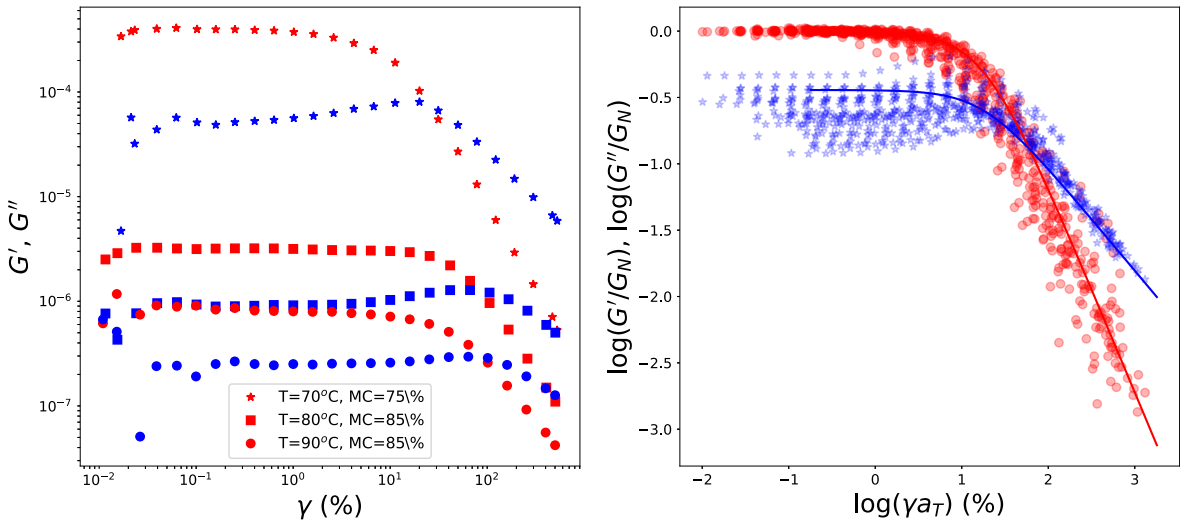

Fig. 4. Left pane: exemplary upward strain sweeps, and Right pane: the master curve of the upward strain sweep of pea protein. With G' in red, G'' in blue. Solid lines are fitted to the superposed experimental data following the descriptive model in Eq. (1), with $a = 1.5$, $n = 0.22$, $\gamma_{cr} = 18\%$. Horizontal and vertical shift factors are shown in Fig. 5.

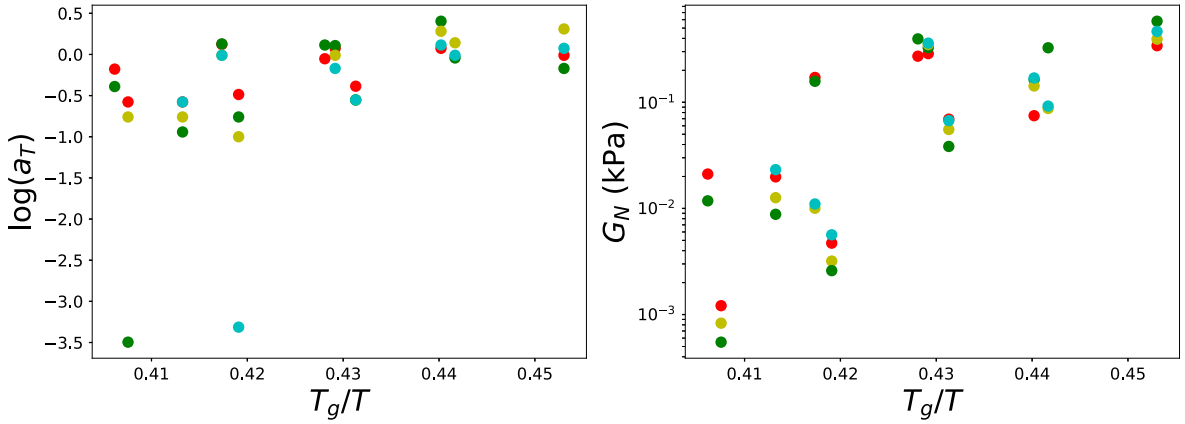

Fig. 5. Horizontal (a_T) and vertical (G_N) shift factors as function as T_g/T as obtained from the upward strain sweeps of pea proteins. Data for the various frequencies are indicated with different colors, which follow the order of the rainbow. Reference conditions are $T_{ref} = 70^oC$, $MC = 80\%$, and $f = 1$ Hz.

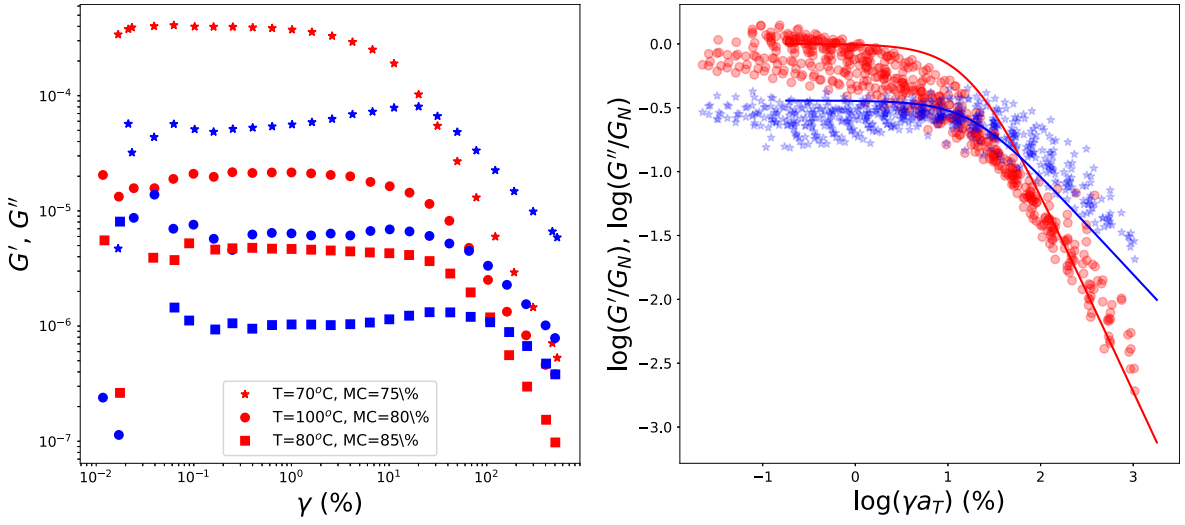

Fig. 6. Left pane: exemplary upward strain sweeps, and Right pane: the master curve of the downward strain sweep of pea protein, with G' in red, G'' in blue, and the complex modulus G^* in black. Solid lines indicate the fit applied to the upward sweep, as shown in Fig. 4.

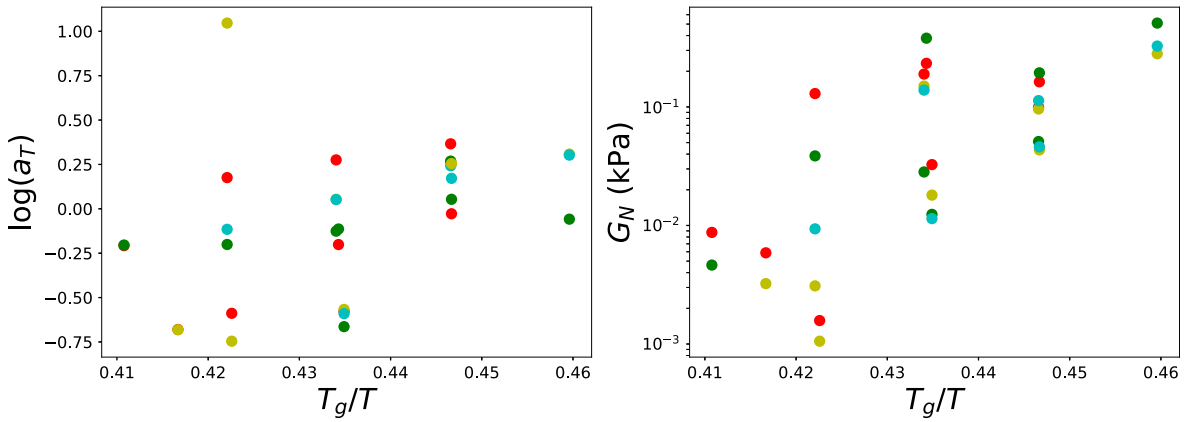

Fig. 7. Horizontal (a_T) and vertical (G_N) shift factors as function as T_g/T obtained from the downward strain sweep of pea proteins. Data from different frequencies are color-coded following the order of the rainbow. Reference conditions are $T_{ref} = 70^oC$, $MC = 80\%$, and $f = 0.5$ Hz.

Differences are due to values of G_N, which still appear to depend on T_g/T, albeit with a lot of variation.

A comparison of the upward and downward amplitude sweeps shows that the pea protein paste does not fully recover. The recovery is defined as the ratio of the elastic modulus in the LVE regime obtained from the downward and upward sweeps of the same formulation:

$$Recovery = \frac{G_{N,down}}{G_{N,up}} \tag{8}$$

The recovery is plotted as a function of T_g/T in Fig. 8. It shows that the recovery is about 40–60%, with a slight dependency on T_g/T.

3.1.2. Soy proteins

For soy protein strain sweeps were performed at different temperatures 70, 80, 90^oC, and 15, 20% of solids. Sweeps are performed at a frequency of 0.5 Hz. This choice of frequency is based on the experience with pea protein isolate, as described previously. Measurements at lower frequencies showed more consistent behaviour. 0.5 Hz is chosen over 0.1 Hz because of the lower total measurement time.

Using the data from the sweep from low to high strain (up-sweep), a master curve is constructed via normalizing G' and G'' with the average elastic modulus in the linear regime $0.1 < \gamma < 1\%$, and somewhat horizontal shifting. The master curve, as shown in Fig. 9, is fitted to the model presented in the theoretical section. The data are fitted with $\gamma_{cr} = 12\%$, $a = 1.5$, and $n = 0.175$ values which are very comparable to the

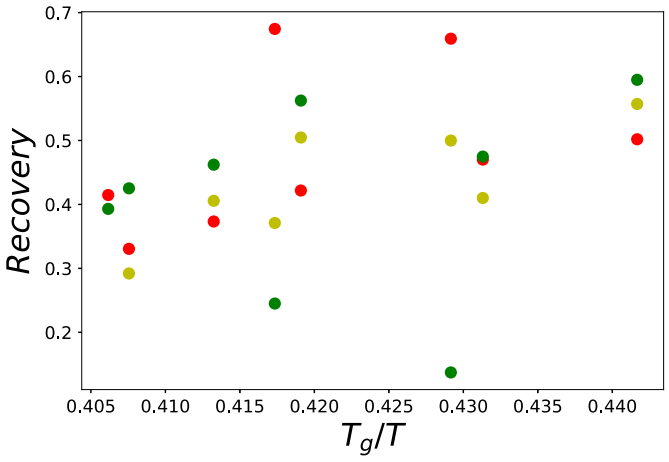

Fig. 8. Recovery of LVE elastic modulus after upward and downward amplitude sweeps (as shown in Figs. 4 and 6, calculated as the ratio of G' in the LVE region. Data is shown for pea proteins and frequencies in range {0.1, 0.5, 1.0} Hz (red to green).

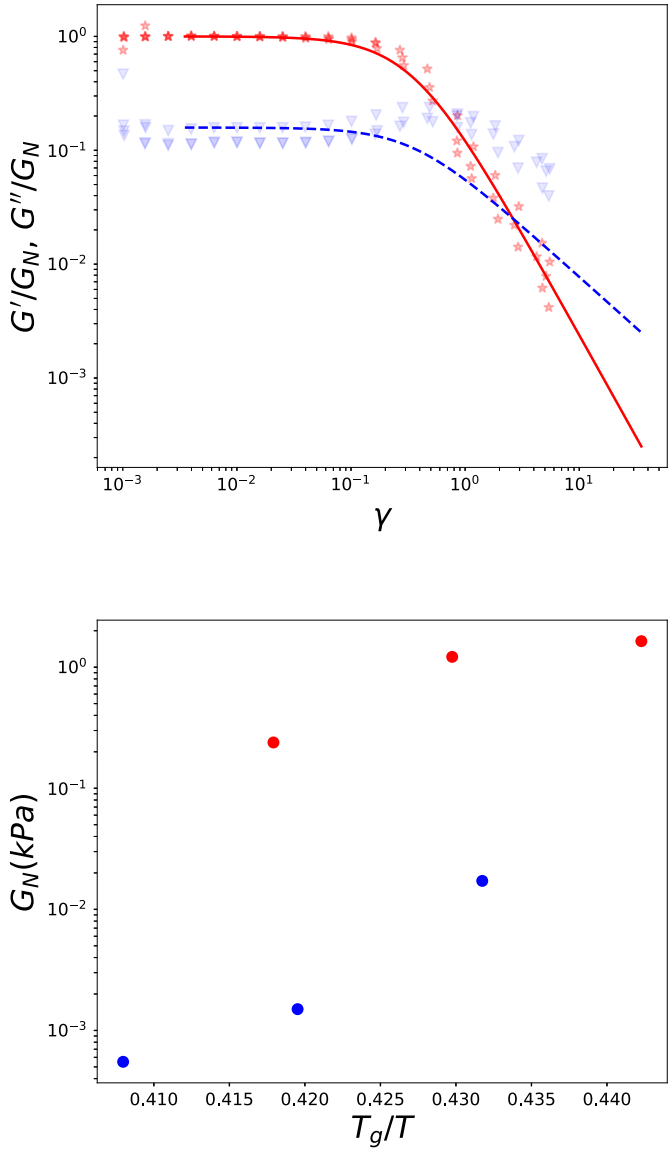

Fig. 9. Top pane shows the master curve of the upward strain sweep of soy protein, with G' in red, G'' in blue lines are fitted following the model in Eq. (1), with $a = 1.5$, $n = 0.175$, $\gamma_{cr} = 12\%$. The bottom pane shows the scaling of plateau modulus G_N with T_g/T with red indicating $y_w = 0.80$, and blue $y_w = 0.85$.

ones of pea proteins. The strain softening index n is related to $\tan(\delta) = \tan(n\pi/2)$. Contrary to pea proteins, is observed a clear weak strain overshoot in Fig. 9, leading to a deviation of G'' from the model. Currently, it is still not clear what exactly causes the weak strain overshoot (Donley, Singh, Shetty, & Rogers, 2020). It is often observed for yield stress fluids, near the transition from solid-like to fluid-like behaviour, i.e. at the crossover point - as is also shown in Fig. 9. Because of the lack of consensus on the overshoot, we refrain from speculating about it.

The vertical shift factors G_N are plotted as a function of T_g/T in Fig. 9. Again, the horizontal shift factor $a_T \approx 1$ (Data not shown). There is some scatter in the plateau modulus versus T_g/T, but it increases with T_g/T for each moisture content.

3.2. Flow curves

3.2.1. Pea proteins

A typical result from a single experiment is shown in Fig. 10 with $T = 70^oC$ and 20% pea protein. For the first upward sweep, is observed that there is not a uniquely defined yield stress, already the structure is being broken down at low shear rates. The other curves clearly show yield stresses. The decrease of the yield stress with each new cycle indicating that the protein pastes are having hysteresis related to thixotropic effects. This means each subsequent cycle leads to further structural breakdown. Beyond a shear rate of $\dot{\gamma} \approx 1\ s^{-1}$, shear thinning appears, which is fully developed for shear rates $\dot{\gamma} > 100\ s^{-1}$. In this regime, the upward and downward sweep of the first cycle overlap. For the other samples, similar behaviour is obtained.

Master curves are constructed for the first downward sweep, and the second upward sweep, which are shown in Fig. 11. The Herschel-Bulkley model can be fitted to the experimental data shear-thinning exponent $m = 0.55$, and critical shear rates of $\dot{\gamma}_{cr} = 60$ and $40\ s^{-1}$ for the downward and upward sweep respectively. The horizontal (a_T) and vertical σ_Y shift factors are shown in Fig. 12. There is too much scatter, to state with statistical confidence there is an inverse relation between horizontal and vertical shift factors.

3.2.2. Soy proteins

Typical results of the flow curves for soy protein with $T = 70^oC$ and $MC = 80\%$ is shown in Fig. 13. Similar behaviour is observed with pea proteins, but soy proteins are showing more instability/erratic behaviour for the upward sweeps. Also yield stresses, as obtained from the downward sweeps, decrease with the number of cycles. This erratic behaviour is probably caused by wall slip, insufficient mixing and/or hydration, or that protein aggregation/breakdown has not reached a steady state (Lapasin, Papo, & Rajgelj, 1983). In our recent review paper van der Sman and van der Goot (2023), we argued that thermomechanical treatment of protein isolates (like PPI and SPI) leads to breakdown of protein aggregates towards building blocks of 25 nm. At high moisture content, the thermomechanical input during pretreatments and shearing of the first cycle are probably too low to obtain the *steady state* of smallest aggregates. Yet, at the end of the first upward sweep, the high shear has fully broken down the microstructure, which offers a better-defined initial state for the rheological characterization of the protein paste.

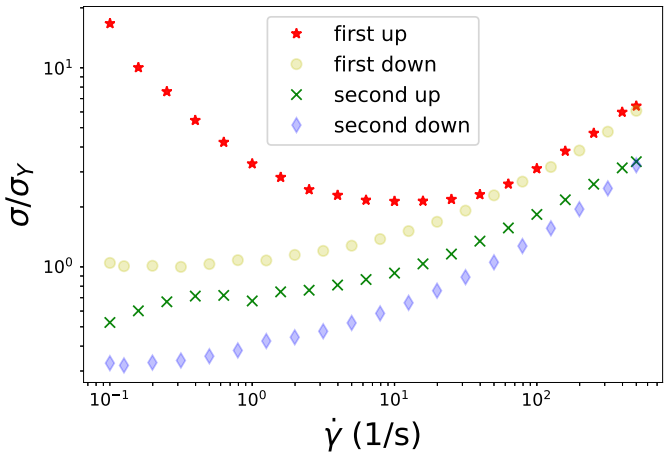

Fig. 10. Example of the two cycles of flow curve measurements of pea protein, for $T = 70^oC$ and MC = 80%.

Master curves are constructed for the first downward sweep, and the second upward sweep, which are shown in Fig. 14. The Herschel-Bulkley model can be fitted to the experimental data but with $m = 0.55$ and $m = 0.6$ for the first downward and second upward sweep respectively. Critical shear rates are $\dot{\gamma}_{cr} = 40$ and $20\ s^{-1}$ for the downward and upward sweep. The horizontal (a_T) and vertical σ_Y shift factors are shown in Fig. 15. There is quite less scatter compared to the case of pea, now indeed indicating an inverse relationship between horizontal and vertical shift factors.

3.3. Inline and capillary rheometry

The steady shear behaviour of SPC via inline and capillary rheometry is discussed next. Via optimization routines based on least squares attempts for superposition of the experimental data were performed. Optimal results are obtained for the following linear relation for the shift factor:

$$\log(a_T) = -1.0\frac{T_g}{T} + 1.1 \tag{9}$$

The individual capillary rheometry results and the superposed data from both capillary and inline rheometry are shown in Fig. 16. For the shift factor we used $T = 100^oC$, and $MC = 55\%$ are reference conditions where $a_T = 1$. It is observed that there is quite some scatter in the individual data of both the capillary and in-line rheometry. Via the rescaling, we show that the magnitudes of our data are in agreement with previous data, but it is difficult to perform model fitting to individual results.

Fitting is only performed to the superposed data, where a power law is used:

$$\sigma = K\dot{\gamma}^m \tag{10}$$

resulting in a shear-thinning index of $m = 0.35$. The master curve is also compared to literature data obtained from capillary rheometry on SPI (Bengoechea, Arrachid, Guerrero, Hill, & Mitchell, 2007; Hayashi et al., 1993). These data indicate a similar shear-thinning index.

4. Discussion

The master curves of the strain sweeps of this study, our previous study, and that of literature on similar systems (Klost & Drusch, 2019) are superimposed on each other, to investigate the consistency between studies. Results are shown in Fig. 17. In the linear regime, and for the strain softening regime at large strains the results from various studies are well in agreement with each other. However, in the transition regime between LVE and the strain softening regime, there is quite some inconsistency. While there is no evidence for this inconsistency, history dependence can play an important role. Above, we have shown that via the strain sweeps cycles pea proteins exhibit hysteresis, and thus the rheology of protein paste is sensitive to their flow history.

To check for consistency of the T_g/T scaling of the classical rheometry data, we have collected the data of G_N from this and our previous study. Results are provided in Fig. 18. The two data sets from the different studies are seemingly consistent, as there appears to be no discontinuity in the relation of G_N with T_g/T. However, it seems that two regimes can be identified, where $\log(G_N)$ scales with a different gradient

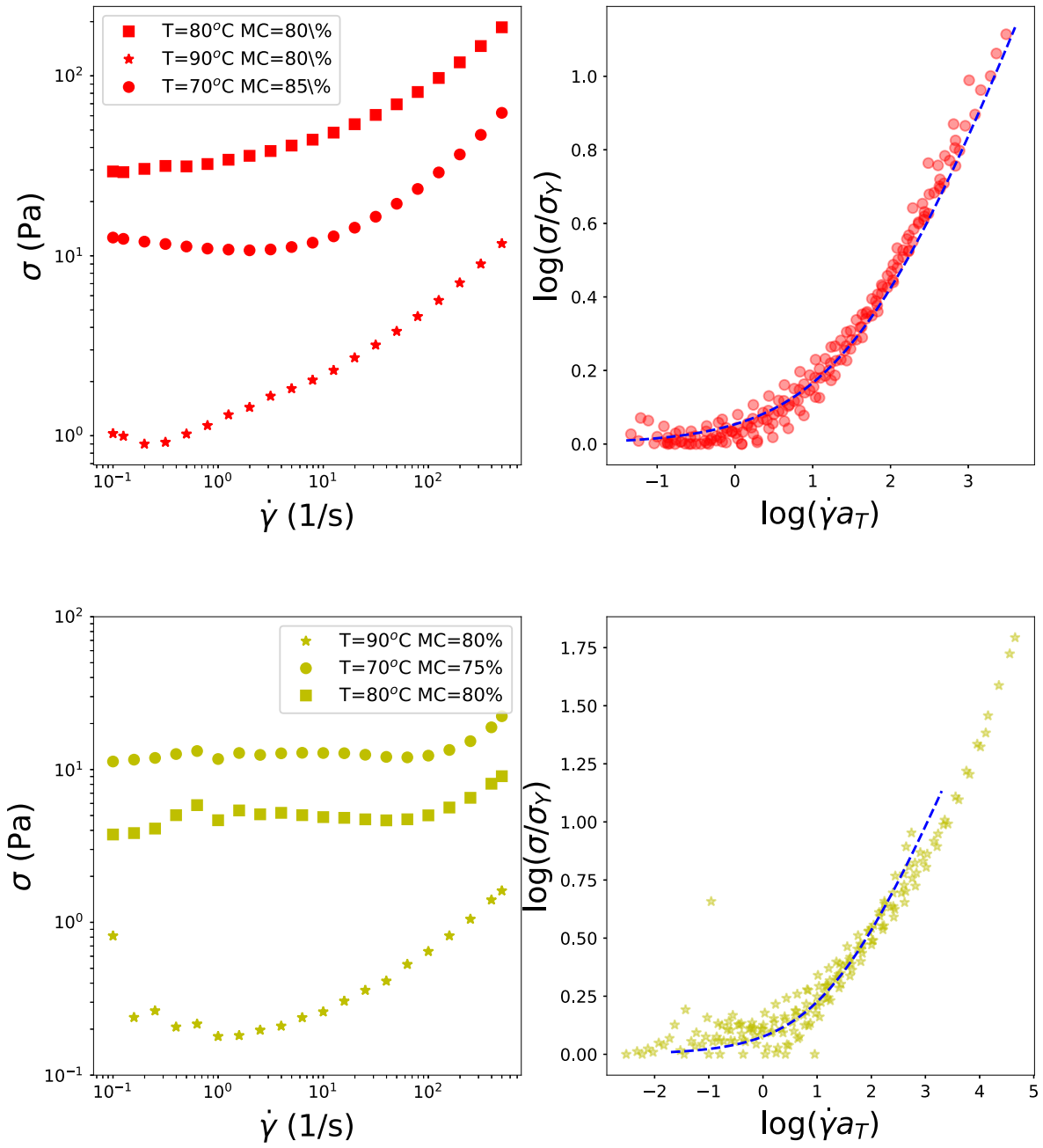

Fig. 11. Examplary flow curves (left) and master flow curve (right) for pea proteins, generated from a) first downward sweep (upper pane), and b) second upward sweep (lower pane). Both master curves are fitted with the Hershel-Bulkley model, with a shear-thinning exponent of $m = 0.55$. The critical shear rate differs slightly ($\dot{\gamma}_{cr} = 40$ vs $20\ s^{-1}$).

against T_g/T. The transition seems to occur around $T_g/T \approx 0.45$. We note, that our previous study has data in the regime $T_g/T < 0.45$, but these samples have been preheated at 120 °C, instead of 90°C for the other samples.

Recent studies indicate that this hysteresis can be due to temperature or T_g/T dependent (Snel, Amroussi, van der Goot, & Beyrer, 2023). Experiments on which extruded SPI pastes were fed back to the extruder, showed similar texture and anisotropy as in the first extrusion - indicating probably little to no hysteresis at more intense thermomechanical treatment. Contrary, extruded PPI doughs did show a degradation in texture after a second extrusion, indicating that thixotropic behaviour is dependent on the type of protein (van der Sman & van der Goot, 2023). During thermomechanical treatment, there is the assumption that protein aggregates are broken down into small units, which reassemble to protein fibers during subsequent cooling (Snel et al., 2023; van der Sman & van der Goot, 2023). The preheating at 90° before rheological measurement is aimed to give sufficient thermomechanical treatment but may be too limited, and render an insufficient breakdown or alignment of protein aggregates, which could be reflected in the change of the gradient of G_N versus T_g/T. The magenta symbols in Fig. 18, related to samples from our previous study preheated at 120°C, seem to indicate that intenser pretreatment does lead to proper aggregate breakdown and alignment. We argue here that the high moisture content of the protein doughs in the current study also may prevent proper aggregate breakdown. This hypothesis is strengthened by observation in another study (Tingle, McClintic, Zervoudakis, Muhialdin, & Ubbink, 2023), where pea protein dough are extruded in a microcompounder. At high moisture contents ($MC > 60\%$) the pea protein dough received poor

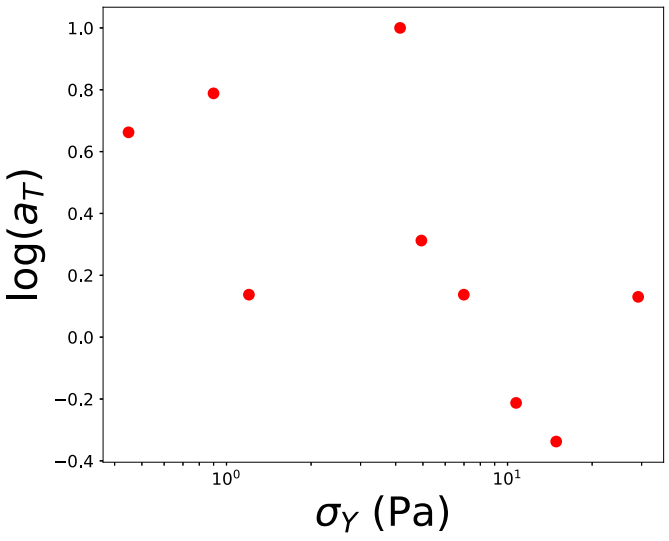

Fig. 12. Horizontal versus vertical shift factors (a_T versus σ_Y) as follows from the construction of the (first downward) master curve for pea proteins in Fig. 11.

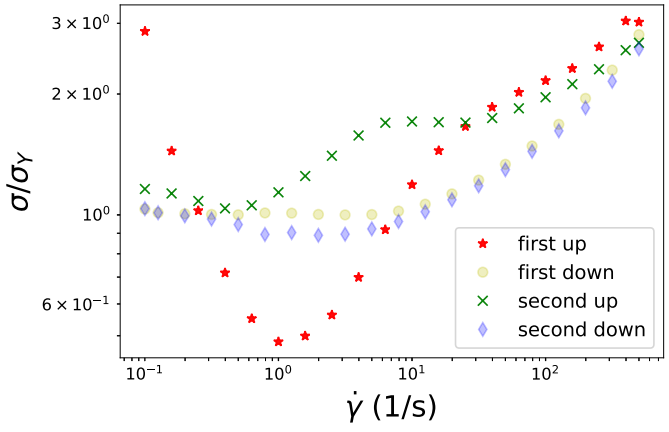

Fig. 13. Example of the two cycles of flow curve measurements for soy proteins, for $T = 70^oC$ and MC = 80%.

thermomechanical treatments, which was attributed to wall slip. Microscopy of the high moisture doughs showed a heterogeneous structure, showing pockets of less bound water. It is stated that moisture content must be significantly below the so-called water holding capacity (WHC). The WHC is a measure of how much water a biopolymer network can absorb when suspended in pure water (Cornet, van der Goot, & van der Sman, 2020). Thus if the moisture content exceeds the WHC, there are expected pockets of free water. Probably, if the moisture content is just below the WHC, the protein paste structure is already heterogeneous, and water is easily expelled from the matrix by stresses, as occurs in extruders or rheometer, leading to water migration to the wall, where the lubrication water layer provides (apparent) wall slip. WHC of pea protein paste is reported to be approximately 3 g/g (Snel et al., 2023; Tingle et al., 2023). This means that the moisture contents of the protein pastes used for the classical rheometers exceed the WHC. Hence, they would have had a consistency more similar to concentrated protein suspensions/pastes, with pockets of free water in between protein aggregates. This structure would probably also explain the observed slip during the first cycle(s) of the flow curve. Another contribution of wall slip might be the small amount of fat present in the protein isolates and concentrates.

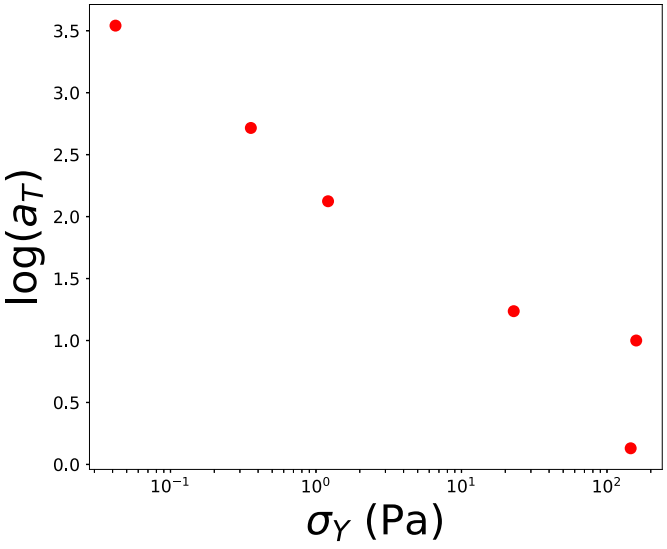

Fig. 15. Horizontal versus vertical shift factors (a_T versus σ_Y) as follows from the construction of the (downward) master curve for soy proteins in Fig. 14.

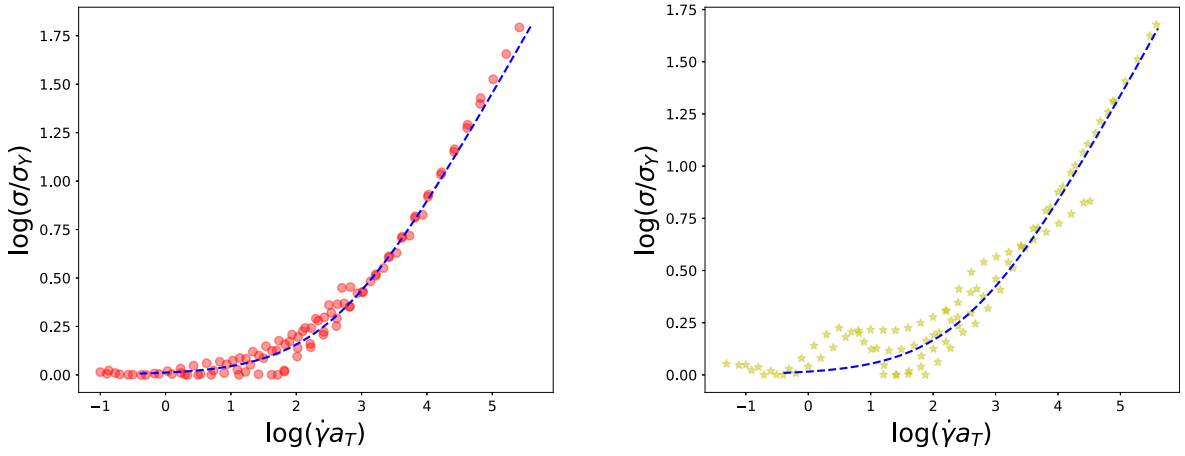

Fig. 14. Master flow curve for soy proteins, generated from a) first downward sweep (left pane), and b) second upward sweep. Both master curves are fitted with the Hershel-Bulkley model, with a shear-thinning exponent of $m = 0.55$ (downward) and $m = 0.60$ (upward). The critical shear rate differs slightly ($\dot{\gamma}_{cr} = 40$ vs $20\ s^{-1}$) (downward vs. upward).

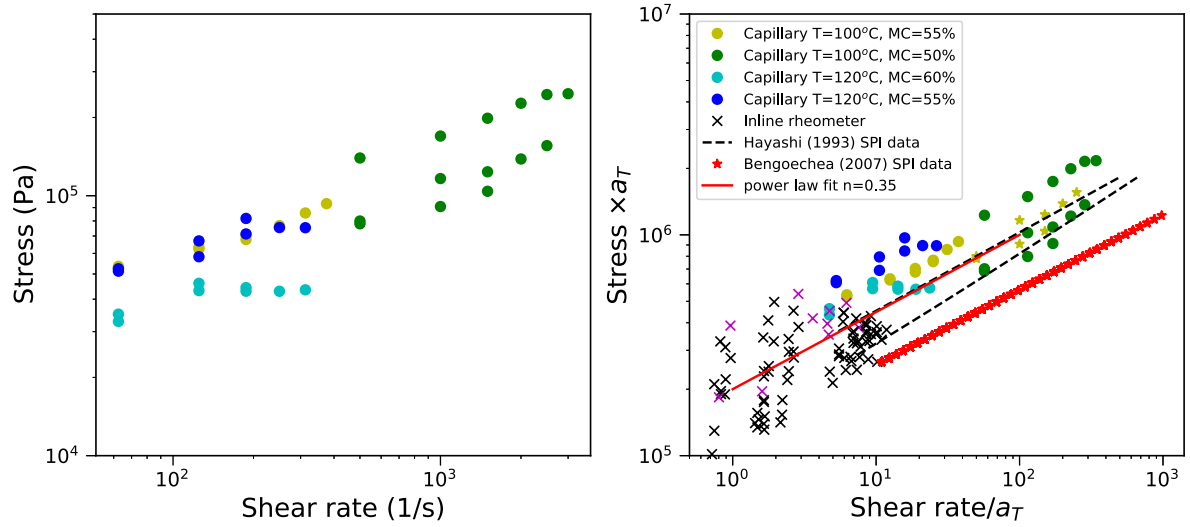

Fig. 16. Left pane: individual flow curves for SPC capillary rheometry, and right pane: superposition of experimental data from steady shear rheology of SPC, as measured with capillary and inline rheometers. The superposed data is fitted by the solid red line, indicating a power law with $m = 0.35$. Our data is also compared to other experimental data on SPI.

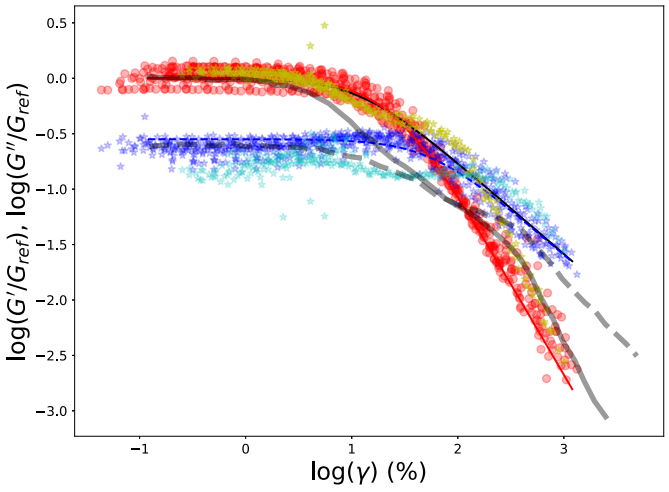

Fig. 17. Superimposed master curves of strain sweeps for pea proteins of this study (red and blue), our previous study (yellow and cyan), and from (Klost & Drusch, 2019) (transparent black lines).

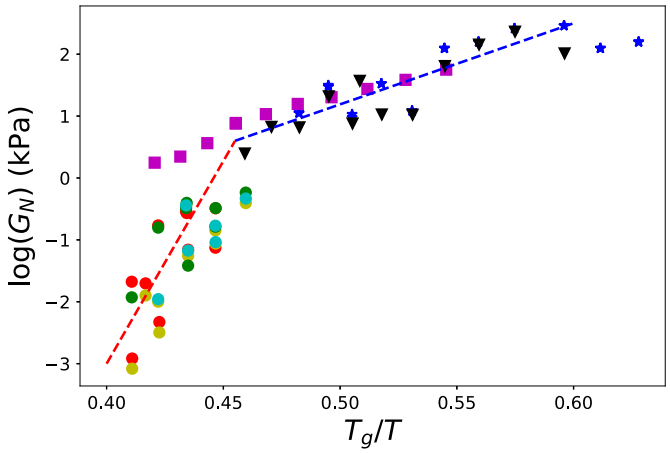

Fig. 18. Plateau modulus G_N from frequency and strain sweeps for pea proteins as a function of T_g/T. Magenta and black symbols are from the strain sweep of our previous study, and the blue symbols are from the frequency sweep of the previous study. All samples received preheating at 90°C, except for the magenta symbols, which are preheated at 120°. Other symbols are from this study, reproduced from Fig. 5. The dashed lines are intended to guide the eye, indicating two possible regimes. For $T_g/T < 0.46$ $\log(G_N) \sim 47\ T_g/T$, while for $T_g/T > 0.46$ $\log(G_N) \sim 14\ T_g/T$.

For soy protein isolate (SPI), the current data of G_N are compared versus T_g/T with data from our previous study, as shown in Fig. 19. The data from the previous study scales as $\log(G_N) \sim 20\ T_g/T$, somewhat higher than the scaling rule for pea protein isolate (for the range $T_g/T > 0.45$). Our new data for $y_w = 0.80$, seem to have a similar gradient, but for $y_w = 0.85$ the scaling factor is higher, similar to the scaling of pea proteins, as measured in the current study with $T_g/T < 0.45$. The latter result strengthens the supposition that at high moisture contents ($y_w \geq 0.8$) moisture is not fully absorbed by the protein matrix, leading to the heterogenous microstructure of individual protein aggregates and pockets of free water, leading to a low elastic modulus, and insufficient structure formation.

Next, we discuss the results of the capillary and inline rheometry. The scaling factor a_T applied to the stress from the capillary rheometry of SPI and SPC, (as shown in) Fig. 16), has surprisingly a much weaker dependency on T_g/T than G_N, as obtained from frequency and strain sweeps, as shown in Fig. 19. This large difference is attributed to wall slip effects. If protein dough is stressed, water can be pressed out, which can form a lubrication layer along the capillary wall - leading to slip.

Wall slip is also attributed to capillary rheometry of SPI plastics (Ralston & Osswald, 2008), and mozzarella cheese (Muliawan & Hatzikiriakos, 2008), where wall slip occurred at stress exceeding 30 kPa. The characteristics of the meat analog protein pastes have a lot of similarities with mozzarella systems (van der Sman & van der Goot, 2023). In the capillary measurements, the data exceeds this limit, and thus the occurrence of wall slip is very likely. Expulsion/migration of water under high stresses can be explained via the Flory-Rehner theory, connected to the WHC of biopolymers (Van der Sman, 2012, 2015). As stress is exerted on the protein paste, like stresses applied during the centrifugation experiment, extra water is expelled from the matrix (shown in the supernatant).

From this general discussion, is concluded that it is difficult to achieve reliable rheological data of meat analog protein pastes under steady shear conditions, which holds for both classical rheometers and capillary rheometers. As argued above, both types of rheometry are plagued by

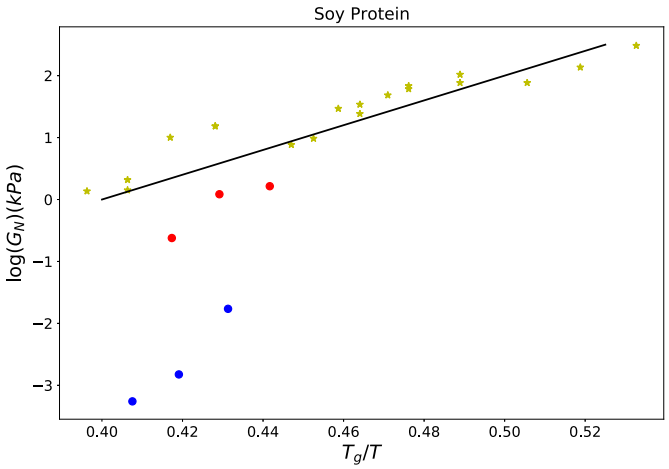

Fig. 19. Plateau modulus G_N from frequency and strain sweeps for soy proteins as a function of T_g/T. Yellow symbols are from the frequency and strain sweeps of our previous study, and the red and blue symbols are from the present study (reproduced from Fig. 9. All samples received preheating at 90°C. The solid line is fitted to the data of the previous data, with $\log(G_N) \sim 20\ T_g/T$.

wall slip. Due to the lower torques provided by the classical rheometers, they are limited to measurements at high moisture content, which often exceeds the WHC limit of the particular protein dough. We hypothesized that wall slip is due to the migration of excess water to the wall, forming a lubricating layer. A similar mechanism can lead to the wall slip in capillary rheometers. The high stresses at the constriction lead to the migration of water.

The difficulty of obtaining reliable steady shear rheometry has recently also been recognized by other researchers (Ellwanger, Georgantopoulos, Karbstein, Wilhelm, & Azad Emin, 2023). That study investigated a new protocol for CCR to estimate the viscosity under steady shear, using simple synthetic polymers. Another possible alternative is shown by Tingle et al. (2023), where viscosities of protein doughs can be measured with a microcompounder with dough moisture contents below their WHC, but at temperature and shear conditions similar to high moisture extrusion. A power law model could be fitted to their data. But, as in the case of capillary rheometry, these measurements can not provide information on yield stresses. For yield stresses we have to rely on CCR data, assuming that $\sigma_Y = G_N\gamma_{cr}$.

5. Conclusions

In this study, the rheology characteristics of plant protein pastes, at temperatures below boiling point, to investigate how consistent the rheology is in this temperature range, compared to rheology at temperatures above boiling point. The latter is often only possible with special rheometers like a Closed Cavity Rheometer (CCR) or a capillary rheometer.

At temperatures below boiling point, both oscillatory strain sweeps were performed as well as flow curves, with the latter more representative of the steady shear conditions in the extruder and cooling die. In one way it was possible to construct master curves from the results, following scaling rules depending on T_g/T, as also found in our previous study. The plateau modulus G_N from the LVE region also scales with T_g/T. The strain softening index n and shear thinning index m are both independent of moisture and temperature. The critical strain, demarking the transition between LVE and strain softening regions, is also independent of both temperature and moisture content. Soy protein pastes show a clear weak strain overshoot, while in pea proteins it is either absent or very small. All protein pastes show hysteresis related to thixotropy, as indicated by the recovery of G_N by only about 50%. The recovery depends on T_g/T. For intensive thermomechanical treatments, the thixotropic effects disappear (Snel et al., 2023).

The thixotropy is likely to cause instability of the flow curve, at increasing shear rates. However, the flow curves at decreasing shear rates are sufficiently stable to construct master curves, with the shift factor for the stress, inversely proportional to that of the shear rate. The master curve follows the Herschel-Bulkley model. The horizontal and vertical shift factors for the flow curves are inversely proportional to each other, which is consistent with an independent critical strain γ_{cr}. Contrary to our previous study, we do not find a relation between the shear thinning exponent m, and the strain softening exponent n, neither for pea or soy.

To investigate the consistency of the current data set, obtained at $T < 100^oC$, with previous data obtained at $T \geq 100^oC$ a comparison is made with the scaling of the vertical shift factor of the amplitude sweeps (G_N) with T_g/T. While the data appear to lie on a continuous line, there appears a different scaling of G_N versus T_g/T, which is much weaker at $T_g/T > 0.45$. The current measurements are all in the other regime of $T_g/T < 0.45$. The shape of the amplitude sweep for pea is consistent with our previous study and with other studies from the literature. The strain softening index is very consistent across all studies.

To investigate further the temperature scaling of rheology capillary and in-line rheometry performed using SPC. Measurements with SPI failed due to blockage of the capillaries. Capillary and inline rheometry show a shear thinning index of $m = 0.35$, which is consistent with the available literature on capillary rheometry on SPC and SPI. However, it is not consistent with the flow curves obtained at $T < 100^oC$, where $m = 0.55 \cdot 0.60$ is found. The scaling of horizontal/vertical shift factor with T_g/T is different from our previous CCR measurements with SPI at $T \geq 100^oC$, but also from those performed by Wittek. We attribute this discrepancy to the occurrence of wall slip in the capillary rheometer.

Hence, while the current study does show that various previously found scaling rules do hold, there is still a discrepancy in the temperature behaviour of the shift factor in different regimes, and for different rheological measurements (flow curves vs. amplitude sweeps). The instabilities shown in the upward flow curves indicate that rheological measurements can be hampered by thixotropy and/or wall slip.

Recent studies from the literature indicate that the wall slip is probably induced by the fact that the moisture content is near the water holding capacity of the protein dough, leading to heterogeneity in the dough structure, making it more resemble a protein paste of packed protein aggregates with pockets of excess/free water, which is easily expelled to the wall of extruder/rheometer upon application of stress.

Hence, the challenge remains how to accurately characterize the full rheology of protein dough under extrusion-like conditions. Yield stress can be quantified by the CCR, but shear thinning must be obtained via rheometry at steady shear conditions with devices having low wall slip. Perhaps novel devices like the microcompounder can be helpful in this.

CRediT authorship contribution statement

R.G.M. van der Sman: Conceptualization, Formal analysis, Investigation, Methodology, Software, Supervision, Writing – original draft, Writing – review & editing. **P. Voudouris:** Data curation, Investigation, Methodology, Writing – original draft. **J.R. Hamoen:** Data curation, Investigation, Methodology, Writing – original draft.

Declaration of competing interest

The authors declare there is no conflict of interest.

Data availability

Data will be made available on request.

Acknowledgements

This research is part of the project Plant Promise, which is co-financed by Top Consortium for Knowledge, The Netherlands, and Innovation Agri & Food of the Dutch Ministry of Economic Affairs, the Netherlands, registered under contract number LWV-19027.

References

Bengoechea, C., Arrachid, A., Guerrero, A., Hill, S. E., & Mitchell, J. R. (2007). Relationship between the glass transition temperature and the melt flow behavior for gluten, casein and soya. *Journal of Cereal Science, 45*, 275–284.

Cardinaels, R., Van Puyvelde, P., & Moldenaers, P. (2007). Evaluation and comparison of routes to obtain pressure coefficients from high-pressure capillary rheometry data. *Rheologica Acta, 46*, 495–505.

Corfield, G., Adams, M., Briscoe, B., Fryer, P., & Lawrence, C. (1999). A critical examination of capillary rheometry for foods (exhibiting wall slip). *Food and Bioproducts Processing, 77*, 3–10.

Cornet, S. H., Snel, S. J., Schreuders, F. K., van der Sman, R. G., Beyrer, M., & van der Goot, A. J. (2020). Thermo-mechanical processing of plant proteins using shear cell and high-moisture extrusion cooking. *Critical Reviews in Food Science and Nutrition*, 1–18. https://doi.org/10.1080/10408398.2020.1864618

Cornet, S. H., van der Goot, A. J., & van der Sman, R. G. (2020). Effect of mechanical interaction on the hydration of mixed soy protein and gluten gels. *Current Research in Food Science, 3*, 134–145.

van Der Sman, R. (2013). Predictions of glass transition temperature for hydrogen bonding biomaterials. *The Journal of Physical Chemistry B, 117*, 16303–16313.

Derec, C., Ducouret, G., Ajdari, A., & Lequeux, F. (2003). Aging and nonlinear rheology in suspensions of polyethylene oxide–protected silica particles. *Physical Review E, 67*, Article 061403.

Donley, G. J., Singh, P. K., Shetty, A., & Rogers, S. A. (2020). Elucidating the g''overshoot in soft materials with a yield transition via a time-resolved experimental strain decomposition. *Proceedings of the National Academy of Sciences, 117*, 21945–21952.

Ellwanger, F., Georgantopoulos, C. K., Karbstein, H. P., Wilhelm, M., & Azad Emin, M. (2023). Application of the ramp test from a closed cavity rheometer to obtain the steady-state shear viscosity. *Applied Rheology, 33*, Article 20220149.

Fujio, Y., Hayashi, N., & Hayakawa, I. (1991). Effect of moisture content on flow behaviour of molten soy-protein isolate under an elevated temperature. *International Journal of Food Science and Technology, 26*, 45–51.

Gibouin, F., van der Sman, R., Benedito, J., & Della Valle, G. (2022). Rheological properties of artificial boluses of cereal foods enriched with legume proteins. *Food Hydrocolloids, 122*, Article 107096.

Grabowska, K. J., Tekidou, S., Boom, R. M., & van der Goot, A. J. (2014). Shear structuring as a new method to make anisotropic structures from soy–gluten blends. *Food Research International, 64*, 743–751.

Hayashi, N., Hayakawa, I., & Fujio, Y. (1991). Entrance effect correction on the flow of moisturized soy protein isolate melt in an extrusion viscometer. *International Journal of Food Science and Technology, 26*, 567–574.

Hayashi, N., Hayakawa, I., & Fujio, Y. (1993). Flow behaviour of soy protein isolate melt with low and intermediate moisture levels at an elevated temperature. *Journal of Food Engineering, 18*, 1–11.

Hayashi, N., Noma, K., Hayakawa, I., & Fujio, Y. (1992). Influence of time-temperature history and strain history on the melt rheology of soy protein isolate at an elevated temperature. *International Journal of Food Science and Technology, 27*, 297–304.

Högg, E., Horneber, T., & Rauh, C. (2017). Experimental and numerical analyses of the texturisation process of a viscoelastic protein matrix in a cooling die after high moisture extrusion cooking. *Experimentelle Strömungsmechanik, 25*.

Jebalia, I., Della Valle, G., & Kristiawan, M. (2022). Extrusion of pea snack foods and control of biopolymer changes aided by rheology and simulation. *Food and Bioproducts Processing, 135*, 190–204.

Jia, W., Rodriguez-Alonso, E., Bianeis, M., Keppler, J. K., & van der Goot, A. J. (2021). Assessing functional properties of rapeseed protein concentrate versus isolate for food applications. *Innovative Food Science & Emerging Technologies, 68*, Article 102636.

Klost, M., & Drusch, S. (2019). Structure formation and rheological properties of pea protein-based gels. *Food Hydrocolloids, 94*, 622–630.

Kristiawan, M., Chaunier, L., Della Valle, G., Lourdin, D., & Guessasma, S. (2016). Linear viscoelastic properties of extruded amorphous potato starch as a function of temperature and moisture content. *Rheologica Acta*, 1–15.

Kyomugasho, C., Kamau, P. G., Aravindakshan, S., & Hendrickx, M. E. (2021). Evaluation of storage stability of low moisture whole common beans and their fractions through the use of state diagrams. *Food Research International, 140*, Article 109794.

Lapasin, R., Papo, A., & Rajgelj, S. (1983). Flow behavior of fresh cement pastes. a comparison of different rheological instruments and techniques. *Cement and Concrete Research, 13*, 349–356.

Martin, P. J., Odic, K., Russell, A., Burns, I., & Wilson, D. (2008). Rheology of commercial and model ice creams. *Applied Rheology, 18*, 12913–1.

Miyazaki, K., Wyss, H. M., Weitz, D. A., & Reichman, D. R. (2006). Nonlinear viscoelasticity of metastable complex fluids. *EPL, 75*, 915.

Mohan, L., Pellet, C., Cloitre, M., & Bonnecaze, R. (2013). Local mobility and microstructure in periodically sheared soft particle glasses and their connection to macroscopic rheology. *Journal of Rheology, 57*, 1023–1046.

Morgan, R., Steffe, J., & Ofoli, R. (1989). A generalized viscosity model for extrusion of protein doughs 1. *Journal of Food Process Engineering, 11*, 55–78.

Muliawan, E. B., & Hatzikiriakos, S. G. (2008). Rheology of mozzarella cheese: Extrusion and rolling. *International Dairy Journal, 18*, 615–623.

Pellet, C., & Cloitre, M. (2016). The glass and jamming transitions of soft polyelectrolyte microgel suspensions. *Soft Matter, 12*, 3710–3720.

Pietsch, V. L., Bühler, J. M., Karbstein, H. P., & Emin, M. A. (2019). High moisture extrusion of soy protein concentrate: Influence of thermomechanical treatment on protein-protein interactions and rheological properties. *Journal of Food Engineering, 251*, 11–18.

Ralston, B., & Osswald, T. (2008). Viscosity of soy protein plastics determined by screw-driven capillary rheometry. *Journal of Polymers and the Environment, 16*, 169–176.

Sadare, O. O., Daramola, M. O., & Afolabi, A. S. (2020). Synthesis and performance evaluation of nanocomposite soy protein isolate/carbon nanotube (spi/cnts) adhesive for wood applications. *International Journal of Adhesion and Adhesives, 100*, Article 102605.

Schreuders, F., Sagis, L., Bodnár, I., Erni, P., Boom, R., & van der Goot, A. (2021). Small and large oscillatory shear properties of concentrated proteins. *Food Hydrocolloids, 110*, Article 106172.

Schreuders, F. K., Schlangen, M., Bodnár, I., Erni, P., Boom, R. M., & van der Goot, A. J. (2022). Structure formation and non-linear rheology of blends of plant proteins with pectin and cellulose. *Food Hydrocolloids, 124*, Article 107327.

Siemons, I., Veser, J., Boom, R., Schutyser, M., & van der Sman, R. (2022). Rheological behaviour of concentrated maltodextrins describes skin formation and morphology development during droplet drying. *Food Hydrocolloids, 126*, Article 107442.

van der Sman, R., Chakraborty, P., Hua, N., & Kollmann, N. (2023). Scaling relations in rheology of proteins present in meat analogs. *Food Hydrocolloids, 135*, Article 108195.

van der Sman, R., & Mauer, L. J. (2019). Starch gelatinization temperature in sugar and polyol solutions explained by hydrogen bond density. *Food Hydrocolloids*. https://doi.org/10.1016/j.foodhyd.2019.03.034

van der Sman, R., Ubbink, J., Dupas-Langlet, M., Kristiawan, M., & Siemons, I. (2021). *Scaling relations in rheology of concentrated starches and maltodextrins*. Food Hydrocolloids, Article 107306.

van der Sman, R., & van der Goot, A. (2023). Hypotheses concerning structuring of extruded meat analogs. *Current Research in Food Science*, Article 100510.

Snel, S. J., Amroussi, Y., van der Goot, A. J., & Beyrer, M. (2023). Rework potential of soy and pea protein isolates in high-moisture extrusion. *Foods, 12*, 2543.

Swallow, F. E. (2002). Viscosity of polydimethylsiloxane gum: Shear and temperature dependence from dynamic and capillary rheometry. *Journal of Applied Polymer Science, 84*, 2533–2540.

Tingle, C. F., McClintic, K., Zervoudakis, A. J., Muhialdin, B. J., & Ubbink, J. (2023). Texturization of pea protein isolate by micro compounding. *Food Research International, 163*, Article 112250.

Valle, G. D., Vergnes, B., & Lourdin, D. (2007). Viscous properties of thermoplastic starches from different botanical origin. *International Polymer Processing, 22*, 471–479.

Van der Sman, R. (2012). Thermodynamics of meat proteins. *Food Hydrocolloids, 27*, 529–535.

Van der Sman, R. (2015). Biopolymer gel swelling analysed with scaling laws and flory–rehner theory. *Food Hydrocolloids, 48*, 94–101.

Wittek, P., Walther, G., Karbstein, H. P., & Emin, M. A. (2021). Comparison of the rheological properties of plant proteins from various sources for extrusion applications. *Foods, 10*, 1700.

Wittek, P., Zeiler, N., Karbstein, H. P., & Emin, M. A. (2020). Analysis of the complex rheological properties of highly concentrated proteins with a closed cavity rheometer. *Applied Rheology, 30*, 64–76.